



# Assessment and mitigation of the influence of rising charging demand of electric vehicles on the aging of distribution transformers

Illia Diahovchenko<sup>a,b,\*</sup>, Anastasiia Chuprun<sup>a</sup>, Zsolt Čonka<sup>c</sup>

<sup>a</sup> Sumy State University, Sumy, Ukraine

<sup>b</sup> Institute for Research in Technology, ICAI, Comillas Pontifical University, Madrid, Spain

<sup>c</sup> Technical University of Košice, Košice, Slovakia

## ARTICLE INFO

### Keywords:

Electric vehicles  
Loss of life  
Transformer's aging  
Battery energy storage  
Photovoltaic generation  
Power distribution network  
Reactive power compensation  
Fuzzy logic

## ABSTRACT

The world is currently moving towards more environmentally friendly modes of transport. As a result, the sales of electric vehicles (EVs) are growing exponentially, and the new charging-associated loads are influencing the operation of the power distribution networks and their elements. Given the stochastic nature of the additional load from EVs, it is difficult to predict such a load with analytical methods. In this regard, a fuzzy-logic-based tool to assess the influence of the charging load of EVs on the transformers' aging was developed in the MATLAB-Simulink environment, and the impact of different EV penetrations was simulated and assessed. The fuzzy-logic-based model incorporates the influence of ambient temperature, power quality, and overloads. It comprises a diagnostic part, which warns a user about possible issues by providing actual information about the transformer's state, and a tuning part, which is aimed at optimizing the transformer's load level and the power factor at the secondary voltage side. Moreover, the effectiveness of photovoltaic generation units, shunt capacitor banks and battery energy storage systems, installed at the secondary voltage side, for distribution transformers' service life extension were analyzed. The results show that, for high EV penetration levels, a combined grid reinforcement strategy allows to reduce the loss of life of the transformer by around 3–5 times.

## 1. Introduction

To meet future mobility needs, reduce climate and health-related emissions, and phase out oil dependence, traditional engine technologies must be replaced by more efficient and eco-friendly alternatives, as EVs [1]. At the same time, several countries (e.g., Germany, Denmark, Sweden) have decided to switch their electricity generation from fossil fuels to renewable energy sources, making EVs even more environmentally friendly compared to internal combustion vehicles. Research has revealed evidence that the transition to EVs is of immense importance for the environment, including overall air quality and reducing carbon emissions [2]. EVs, compared to diesel or gasoline-powered cars, produce fewer lifecycle emissions, and these emissions can be further reduced with electricity generated from non-polluting renewables, such as wind and solar. Until now, electric vehicles have been gradually gaining momentum in the market. According to the latest edition of the "Global Electric Vehicle Outlook" from the International Energy Agency [3], in 2021 sales of EVs doubled to a new record of 6.6 million, and the interest kept rising strongly into 2022, despite disruptions in global

supply chains.

### 1.1. Problem statement and motivation

For the electrical distribution network, EVs are primarily an additional load of a stochastic nature, which complicates the process of managing the power system and affects its reliability. For example, EV charging during peak hours increases the total demand in the power system and can lead to the transformer's overloading and disruption of the energy supply [4].

According to [5], up to 4 out of 5 plug-in EVs recharging occasions occur at the residential homes, and about 1 out of 5 charging events take place at the workplace. Typically, the residential homes in Europe are supplied through electric networks, which are tied to distribution transformers. Therefore, this work is focused on the impacts of home charging on the distribution transformers feeding those power networks. Contemporary residential homes are adapted to high-power fast chargers at 10–22 kW as opposed to traditional charging at 3–6 kW [6]. Several fast charging 20 kW connectors operating simultaneously can

\* Corresponding author at: Sumy State University, Sumy, Ukraine.

E-mail address: [i.diahovchenko@etech.sumdu.edu.ua](mailto:i.diahovchenko@etech.sumdu.edu.ua) (I. Diahovchenko).

cause a blackout in a holiday village with transformers that are not designed for such loads. Overrating of a transformer leads to an increase in the temperature of the windings, taps, insulation and oil, which can reach unacceptable values. Also, the induction of the scattering magnetic flux increases, causing an increase in eddy currents that heat the metal parts of the transformer. As a result, there is a risk of damage associated with the amount of current and temperature, and the aging is accelerated.

In parallel with that, harmonic distortions in electric energy systems continue to grow due to the proliferation of nonlinear loads and electronic devices [7]. Moreover, photovoltaic (PV) systems with low short-circuit power can affect the voltage profile and cause harmonic distortion of voltage and current [8,9]. When nonlinear loads are connected to the distribution networks, they tend to draw nonlinear currents and consequently distort the system's voltage [10]. The most substantial effect of harmonic distortions within a power distribution network is the temperature increase, which results in increased power losses, transformer derating and possible equipment failures [11]. In addition to that, harmonic distortions can adversely affect system's microcontrollers, electric energy meters, breakers and relays, causing their erratic behavior [12].

Local power injection from a community-level PV system and from prosumers with rooftop PV panels can help to avoid the transformer's overloading due to EVs charging. However, due to the intermittent nature of PV technologies and the specific generation profile (solar installations usually make their major contribution at noon), the effect on transformer aging would be insufficient [13]. For more efficient transformer's aging mitigation, PV generation should be coupled with battery energy storage systems (BESSs) [14]. Installation of a BESS is most common for single-family homes with PV systems, which gives homeowners the ability to store available surplus of energy during the daytime and consume that energy during times of pick demand or when there is no generation from renewable energy sources [15].

## 1.2. Previous work analysis and contribution

It is commonly assumed that EVs charging often starts after people return from work, which coincides with the evening peak load [4]. This coincident demand of lighting, household appliances and EVs charging can overload the power distribution system, which was initially projected for lower energy demand.

The impact of plug-in EVs charging on the power distribution systems and their elements has been on agendas of many researchers during the recent years. In [4] the authors evaluated home-dominant and work-dominant EV charging impacts on the power grid and reported noticeable line loading increase of about 15%. The work [16] demonstrates that operation of quick charging stations can lead to the increase of the transformer's temperature beyond the thermal limits and reduce its lifetime. The effect of the current and voltage harmonic distortions on the distribution transformer's aging was evaluated in [17]. The study [18] revealed that voltage harmonics can cause significant increase of top-oil temperature rise and core losses of pole-type oil-filled transformers, deterioration the winding insulation. A methodology to obtain spatial and temporal projections of charging demand and to assess the peak-shaving potential from EVs is proposed in [19]. The paper [20] demonstrates a possibility to extend the transformer's life through the optimal scheduling of the EV charging. The authors of [21] investigate whether grid reinforcements are reasonable from a cost and emissions perspective for an electrical network with high penetration of EVs, concluding that it is possible to reduce the EV charging costs under the current transformer's capacity. The article [22] assesses the influence of the stochastic load of electric cars on the distribution network and concludes that EV charging can cause unacceptable voltage decrease in load nodes.

The complexity of modeling the EV charging loads is due to their stochastic nature; therefore, the use of analytical modeling methods is

practically impossible, and different numerical methods are preferred [22]. Evaluation of distributional transformers' aging acceleration as a result of extra charging loads added by plug-in hybrid electric vehicles is given in [23]. Probabilistic data-driven methods to assess the severity of transformer's overloading and aging, when imposed to high-level of EVs charging demand coupled with generation from rooftop PV, are presented in [24,25]. In [26] the thermal aging of oil-immersed transformers is estimated, using an artificial neural network and Monte Carlo simulations. The article [27] proposes to employ a deep learning approach based on a convolutional neural network to predict the life duration of the transformer. The authors of [28] and [29] assessed the transformers' loss of life (LoL) in distribution networks with individual residential houses and high number of plug-in EVs and investigated how the transformer's aging can be mitigated by means of the power system reinforcement, including local PV generation and BESSs. The results of [24,25] have shown that the presence of PV generation in the electrical networks with EV chargers can decrease the transformer's LoL, and with a BESS this positive effect is even more significant [28,29].

In [4,19] the effects of EV charging demand are only investigated for bus voltage and branch loading levels. The papers [16,19–23] study the transformers' deterioration, but the effects of prosumers with rooftop PV panels or options of the electrical network upgrading with BESS units were not considered. The effect of distributed generation and energy storage technologies is not incorporated in the transformer's aging model in [26]. The methods based on the artificial intelligence [26,27] require a large number of data with known conditions for training and testing, but they are still subjective. Additionally, in [27] the characteristic quantities used in the prediction model were obtained assuming their Weibull distribution, which that may not be valid in all cases. To quantify the uncertainties of stochastic processes and calculate expected values of unknown data generating processes, the Monte Carlo method is employed in [22,24–26,28]. This method consists in generating a large number of random values for distributions of quantities given by the corresponding probability densities, on the basis of which the probabilistic characteristics of the problem being solved are calculated [30]. However, the accuracy of Monte Carlo calculations strongly depends on the number of iterations. For instance, to increase the accuracy by 10 times, it is necessary to increase the number of iterations by 100 times. And as the number of iterations increases, so does the calculation time [30]. In [29] only a single level of EV penetration is modeled, while the considered share of reactive power is unrealistically high for a residential power network.

To overcome the limitations of the previous studies, the influence of the ambient temperature variations, EVs charging, and power quality issues on the transformer's aging should be investigated more complexly. This study is based on the outputs of the previous research works [28,29]. Compared to [28], the influence of higher harmonics and shunt capacitor banks (SCBs) on transformers' aging have been incorporated in the modeling, and more case scenarios have been created. Compared to [29], various EV penetration levels have been considered, covering the range of penetration from 0% to 100%, and the potential of PV installations has been employed to control the power factor (PF). The effectiveness of several grid reinforcement strategies for mitigation of the transformer's LoL under different EV penetration levels has been estimated. These strategies include deployment of BESS, dispersed PV generation, and SCBs to compensate the reactive power. A fuzzy-logic-based tool has been set up to prevent overloading and overheating of the mineral-oil-immersed transformer, while maintaining the PF at a desired level. The rules for diagnostics and tuning settings can be adjusted by a user, depending on the rated capacity, voltage level or specific operational conditions. Thus, the proposed approach is applicable for different sites of distribution networks.

The rest of the paper is organized as follows. Section 2 defines the input data and the case study scenarios. Section 3 presents the algorithm and the developed model. The transformer's aging model is defined in Section 4. The obtained results are discussed in Section 5. Some

strategies to prolongate the transformers' life cycle, which do not rely on grid reinforcements, are outlined in Section 6. And next the conclusions are stated.

## 2. Input data for the case study

### 2.1. Power demand in distribution system

A distribution power network, which is typical for power supply of European rural areas, is considered as a research object. A possible configuration of such a network is shown in Fig. 1. The radial feeder is equipped with a 20/0.4 kV mineral-oil-immersed transformer and hosts residential dwellings and a local enterprise. A shunt capacitor bank with a 12-step regulator and a BESS are connected to the secondary voltage bus. The SCB has a capacity to compensate 90% of the maximal reactive power demand. The aggregated size of BESSs units should be 60% of the rated power of all PV generation units, which is sufficient to absorb the surplus of PV power in the electrical network under study. The latter value was determined during the modeling process, and for this estimation a BESS of unlimited capacity was initially embedded in the model.

The hourly transformer's loading at each  $t$ -th sampling step can be calculated as

$$S_{T,t}^{tot} = \sqrt{(P_{Load,t} + P_{EVs,t} - P_{PV,t} \pm P_{BESS,t})^2 + (Q_{Load,t} - Q_{c.b.,t})^2}, \quad (1)$$

where  $P_{Load,t}$ ,  $Q_{Load,t}$  are the  $t$ -th active and reactive power demands of consumers, respectively;  $P_{EVs,t}$  is the  $t$ -th power demand of EVs;  $P_{PV,t}$  is the  $t$ -th solar power output;  $P_{BESS,t}$  is the  $t$ -th BESSs power output/consumption;  $Q_{c.b.,t}$  is the  $t$ -th power output of the shunt capacitor bank. Duration of each sampling step is assumed 1 hour.

For the values  $P_{Load,t}$  and  $Q_{Load,t}$  the electricity demand data of 11 real residential dwellings and a small enterprise is used in this work. The average PF of the cumulative loading from residential and manufacturing consumers is 0.8. The PV and the EV inverters are assumed to have a PF of unity.

To incorporate the  $P_{EVs,t}$  values, the EVs demand charging curve has been replicated from [19]. According to the results of [31], the variance in the EVs' charging behavior across seasons is limited (i.e., there are no specific seasonal patterns), and there is no substantial difference in the start-charging times among weekdays or between weekends. Therefore, for this study two generalized charging curves are used for the whole year: one for weekdays and another for weekends. Charging events for holiday dates are treated as weekdays or weekends, depending on the day of the week the holiday happened. Additionally, it is assumed that EV charging demand on a weekend is about 2/3 times smaller compared to a working day.

The PV electric output,  $P_{PV,t}$  is calculated based on the mathematical model from [32], using the solar irradiation data and the ambient temperature data from the photovoltaic geographical information

system (PVGIS) [33] for the geographical coordinates of Kherson city.

Such a calculation approach is universal and can be applied to any section of the network if there is initial data on this section.

### 2.2. Higher harmonics and temperature

Another two factors to incorporate in the model are the ambient temperature and the power quality. The ambient temperature data for the considered geographical location was taken from the PVGIS [33].

The power quality aspect is represented through the voltage harmonic distortions. The voltage harmonic of the fundamental frequency and higher voltage harmonics have been synthetically generated using a random distribution in the following ranges: 90–110% for the fundamental harmonic; 0–7.5% for the 3rd harmonic; 0–9% for the 5th harmonic; 0–7.5% for the 7th harmonic; and 0–5.25% for the 11th harmonic. These ranges are 1.5 wider, compared to the permissible relative voltage levels established in EN 50,160–2010. In this case it is assumed that the electrical network is polluted with higher harmonics, which can come from manufacturing nonlinear loads, PV inverters and, to an extent, from EV inverters [8,17,18].

The cumulative influence of higher harmonics on the distribution transformer can be indirectly evaluated through the total harmonic distortion (THD) [10]:

$$V_{THD} = \frac{\sqrt{\sum_{h=2}^{\infty} V_h^2}}{V_1}, \quad (2)$$

where  $V_{THD}$  is total voltage harmonic distortion;  $V_h$  is voltage harmonic component in root mean square (RMS);  $V_1$  is a fundamental voltage in RMS.

### 2.3. What-If scenarios

In this work five different scenarios were elaborated. Their description is given in Table 1.

## 3. Algorithm and model description

Designing of a diagnostic tool for power application can be challenging, since it needs to be tuned to a specific system, and usually several measurements need to be taken and compared to obtain reasonable performance [11]. Therefore, the mathematical tool of fuzzy logic has been chosen for to analyze the limit states (overload, temperature overheating) during transformer operation. The fuzzy-based model can operate with input data specified indistinctly; it analyzes the parameters and factors that affect the normal operation of the transformer and helps to anticipate emergencies. Using signals from the fuzzy logic controller, automation acts to prevent the transformer's overloading.

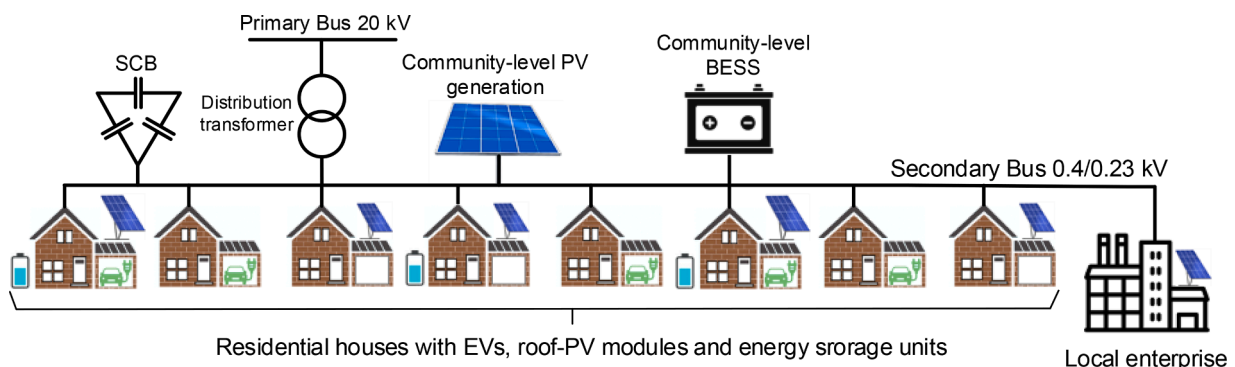


Fig. 1. The secondary distribution system.

**Table 1**  
What-if scenarios for the study.

| Scenario  | Description  |
|-----------|--|
| Base case | The feeder contains only residential and manufacturing loads and EVs. Six EV levels have been considered, namely 15%, 33%, 50%, 67%, 85%, and 100%. The average PF of the loads, excluding EV charging loads, is 0.8.  |
| Case 1    | PV generation units have been added to the electrical network. These can be rooftop PV systems, standalone PV systems or community-level PV systems at the secondary side of the transformer. The installed power of PV units is 100% of the transformer's nameplate rating. The output of the PV generation can be regulated to control the PF. |
| Case 2    | In addition to the PV generation, a regulated shunt capacitor bank has been injected at the secondary bus of the transformer. The capacity of the SCB is 90% of the feeder's reactive power consumption. The output of the SCB can be regulated to control the PF.   |
| Case 3    | In addition to the PV generation and SCB, controlled BESSs have been added. Energy storage can be local (e.g., stationary home energy storage) or community-level, both installed at the secondary side of the transformer.  |

The flowchart in Fig. 2 outlines the steps of implementing the proposed fuzzy-logic-based algorithm. This algorithm is generic for each scenario presented in Table 1, but some blocks can be activated or not in

the process, depending on the studied case.

Once the input data is loaded, parameters of the electrical network, such as aggregated power consumption on the transformer's secondary bus and PF are to be calculated. Next, a fuzzy logic control system for diagnostic of the distribution transformer is to be employed. The left part of the algorithm is dedicated to diagnostics. It consists of a set of input membership functions (MFs), a rule-based controller and a defuzzification process. The MFs are curves that define how each point in the input space is mapped to a membership value between 0 and 1 [34].

The fuzzy logic input uses MFs to determine the fuzzy value of the input [34]. There are different MF topologies available in MATLAB Fuzzy Logic Toolbox, such as triangular, trapezoidal, Gaussian, polynomial, sigmoidal. The voltage harmonic distortion, the ambient temperature, and the transformer's resulting loading are the three inputs to the fuzzy logic system for diagnostics (see Fig. 3), and each input has several MFs. The attributes of the MFs for each input are then manipulated to add weight to different inputs. The Mamdani fuzzy system with the centroid method for defuzzification was selected [35].

The diagnostic system uses randomly generated data for voltage harmonics, as described in Section 2.1. There are three voltage harmonics MFs, which define THD in the range from 0% to 12% as low,

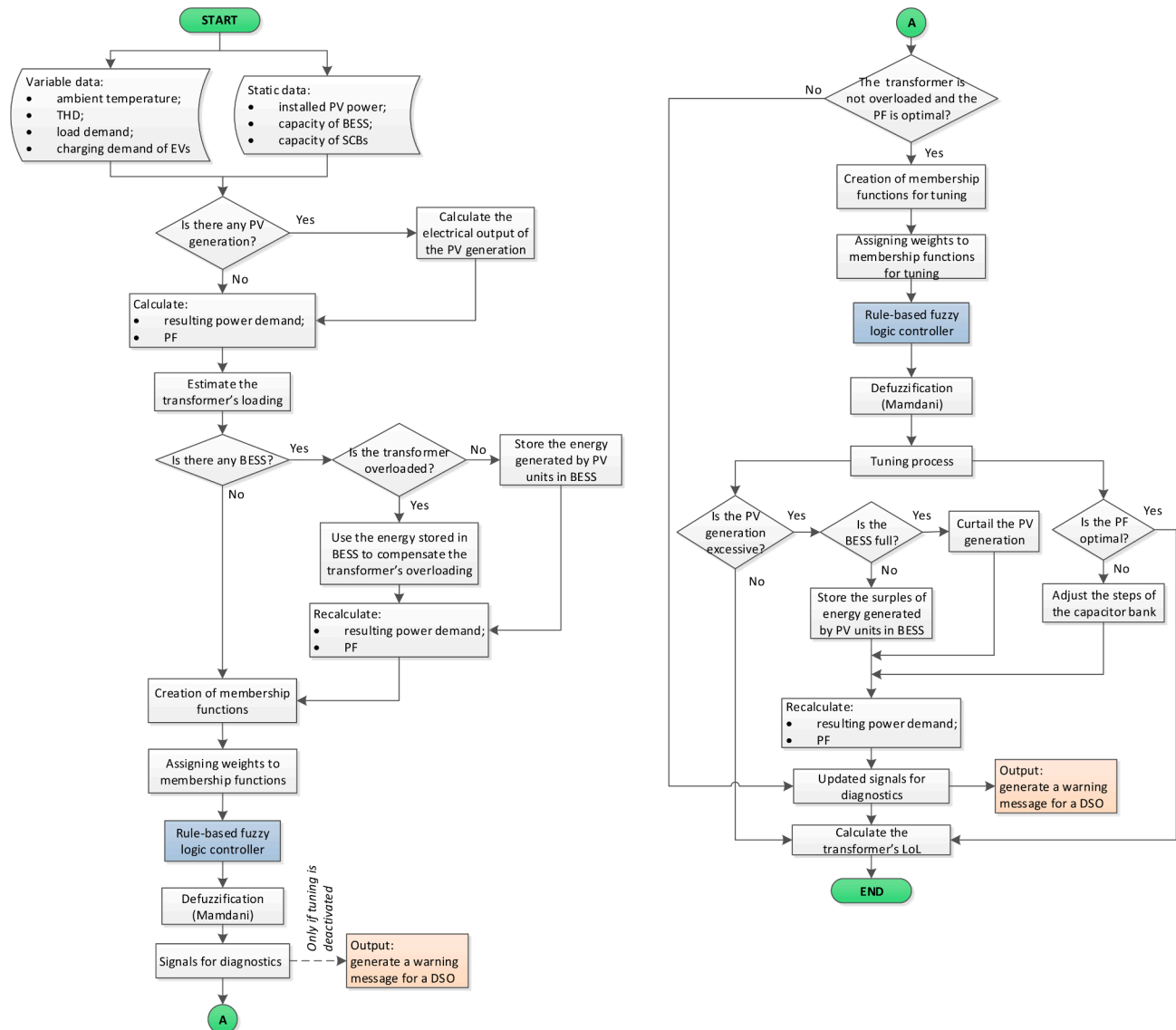


**Fig. 2.** The flowchart of the proposed fuzzy-logic-based approach.

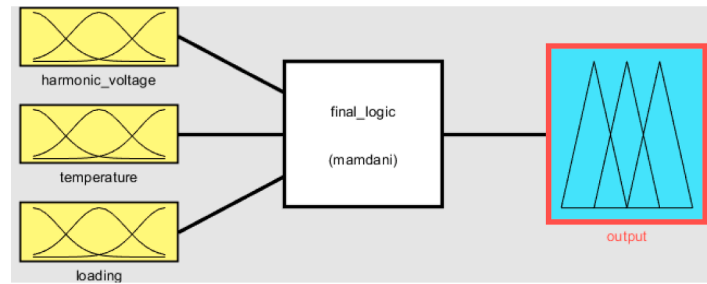


Fig. 3. The fuzzy logic system for diagnostics.

medium or high (Fig. 4a). The ambient temperature has four MFs, laying between  $-25^{\circ}\text{C}$  and  $+50^{\circ}\text{C}$  (Fig. 4b). For the loading (Fig. 4c) there are three input variables, which split the range from 0% to 200% in “low”, “normal”, and “overload” zones. Additionally, the “harmonic voltage” input has a weight of 1, the “temperature” input is weighted 1.15, and the “loading” input is weighted 1.25.

The output also has a set of MFs, which define the possible responses and outputs of the studied system [11]. In the created model there are four output MFs: “No issue”, “Attention”, “Possible issue”, and “Inevitable issue” (Fig. 4d).

The corresponding rule surfaces are demonstrated in Fig. 5.

Next, all the output MFs are combined into one aggregated fuzzy set. A crisp value for representing uncertain data from this aggregated topology is obtained through a defuzzification process.

The rules for the diagnostic part of the algorithm are user-defined and listed in Table 2.

When the fuzzy control system is defined, it can be exported into Simulink model. The inputs are processed by the fuzzy logic controller, the fuzzy output is decoded and split into four ranges, and then an integer from 0 to 3 is output and sent to scopes and to workspace variables. These integers reflect the transformer’s state and can be decoded into a degree of warning message for a distribution system operator (DSO), which are of the following four types: “No issue”, “Attention”, “Possible issue”, “Inevitable issue”. In case of an “Inevitable issue”, an alarm signal can be sent to a distribution system operation center. In such a way, the diagnostic part of the model monitors the state of the

distribution transformer and generates a warning message for a DSO.

The right part of the algorithm (see Fig. 2) is dedicated to tuning. For this purpose, an additional fuzzy logic controller was integrated in the Simulink model. The objectives of tuning are to avoid heavy overloading of the transformer and to maintain the PF around 0.92, whenever possible. These can be implemented by adjustment of the SCB’s reactive power output, by control of charging and discharging modes of a BESS, and by temporary curtailment of PV generation.

The fuzzy logic system for tuning is shown in Fig. 6. It has three inputs, which are data about PV generation, overall apparent power, which depends on the energy demand, and PF at the secondary bus of the transformer. Each input has embedded MFs.

The three “PV power” MFs define the PV generation in the range from 0% to 140% of the transformer’s rated power as low, medium or high (Fig. 7a). The two “cos  $\phi$ ” MFs specify the transition between poor and high PF values (Fig. 7b). The two MFs for the total loading cross in the point of 100% of the transformer’s rated power (Fig. 7c). The three output MFs define the possible responses of the system. Anything from 0 to 0.5 requires a “subtle” tuning, from 0.25 to 0.75 – an “active” tuning, and from 0.75 to 1 – an “intense” tuning (Fig. 7d).

The corresponding rule surfaces are demonstrated in Fig. 8.

Depending on the output value, the system can adjust the SCB’s reactive power output from 0% to 100% (one step is 8.33%), curtail up to 15% of the available PV power output, and switch between charging and discharging modes of the BESS. The tuning is successful if duration of the transformer’s operation under “Inevitable issue”, “Possible issue”,

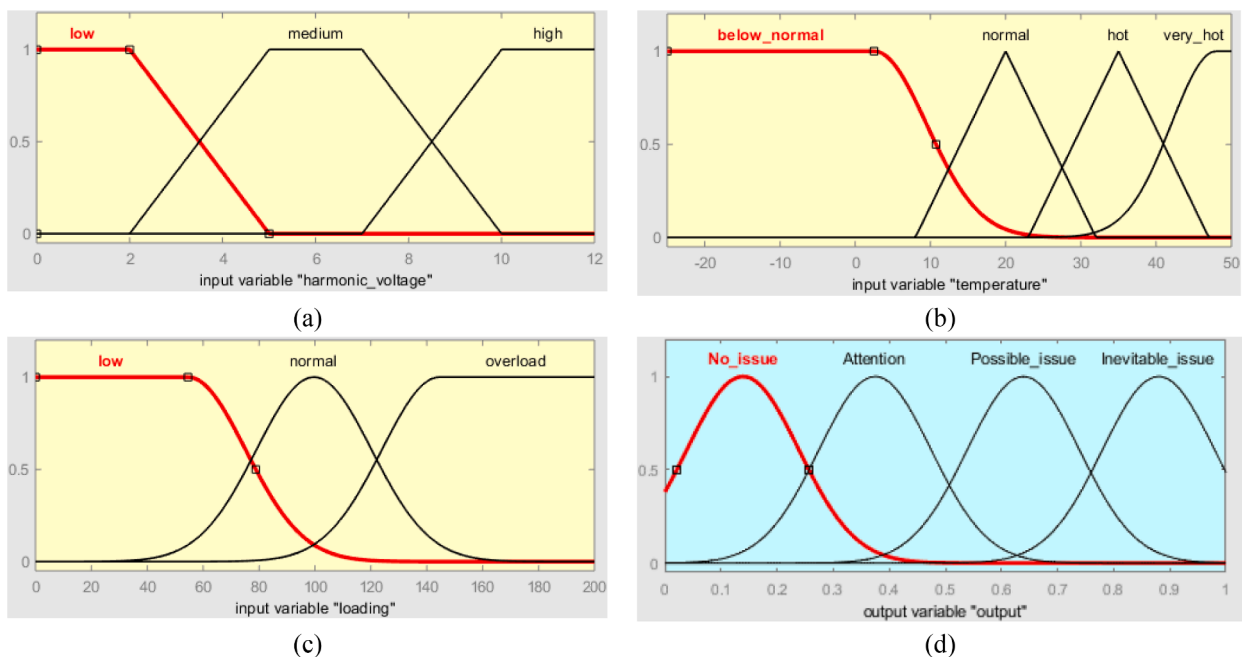


Fig. 4. Membership function plots: (a) voltage THD; (b) ambient temperature; (c) aggregated loading; (d) output of the diagnostics fuzzy logic controller.

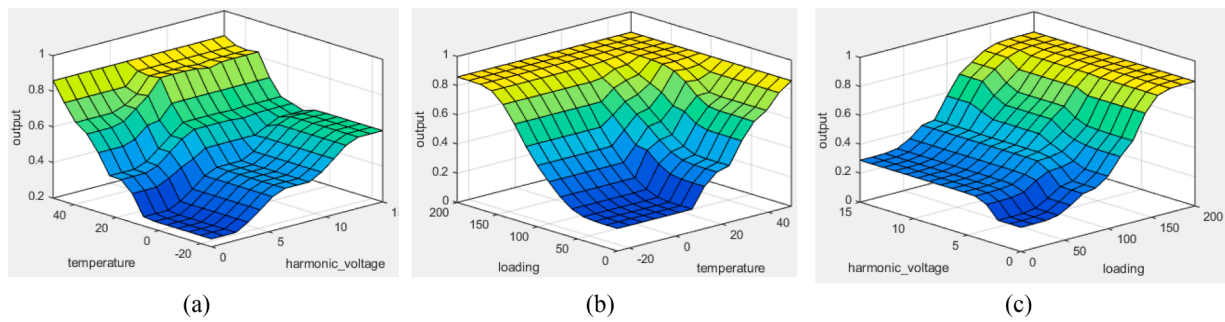


Fig. 5. Fuzzy control rule surfaces for the diagnostic system: (a) dependence of the output from the ambient temperature and the voltage THD; (b) dependence of the output from the ambient temperature and the loading; (c) dependence of the output from the loading and the voltage THD.

Table 2  
Membership rules for the diagnostics part of the algorithm.

| IF the “temperature” is: | AND the “harmonic voltage” is: | AND the “loading” is: | THEN the Output is: |
|--------------------------|--------------------------------|-----------------------|---------------------|
| below normal             | low                            | low                   | No issue            |
| below normal             | low                            | normal                | No issue            |
| below normal             | medium                         | low                   | No issue            |
| below normal             | medium                         | normal                | Attention           |
| below normal             | high                           | low                   | No issue            |
| below normal             | high                           | normal                | Possible issue      |
| normal                   | low                            | low                   | No issue            |
| normal                   | low                            | normal                | Attention           |
| normal                   | medium                         | low                   | Attention           |
| normal                   | medium                         | normal                | Possible issue      |
| normal                   | high                           | low                   | Attention           |
| normal                   | high                           | normal                | Possible issue      |
| hot                      | low                            | low                   | Attention           |
| hot                      | low                            | normal                | Possible issue      |
| hot                      | medium                         | low                   | Possible issue      |
| hot                      | medium                         | normal                | Inevitable issue    |
| hot                      | high                           | low                   | Possible issue      |
| hot                      | high                           | normal                | Inevitable issue    |
| very hot                 | –                              | –                     | Inevitable issue    |
| –                        | –                              | overload              | Inevitable issue    |

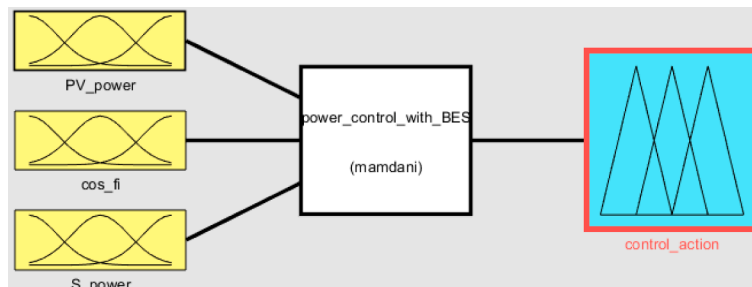


Fig. 6. The fuzzy logic system for tuning.

and “Attention” conditions is minimized in favor to the “No issue” condition. If transition to the “No issue” state is impossible, sledding to a less threatening regime, would be preferable.

The rules for the tuning part of the algorithm are user-defined and listed in Table 3.

The model based on the fuzzy-logic-based algorithm was implemented in the MATLAB-Simulink environment, as shown in Fig. 9. The tuning part is dashed with a green line, and the rest of the blocks belong to the diagnostic part. The presence of particular elements, required by

the algorithm Fig. 2, in the model is determined by positions of the switches, which are enumerated from 1 to 5 in Fig. 9. The switches can activate/deactivate certain blocks and enable/disable control options, depending on the studied scenario.

The input data about the EV charging demand, load demand, PV generation, and shunt capacitor bank is received from the corresponding signal builders, aggregated and sent to the MATLAB S-function “s\_func\_calc\_power,” which calculates the transformer’s loading and the PF at each sampling step. The synthetically generated data about the

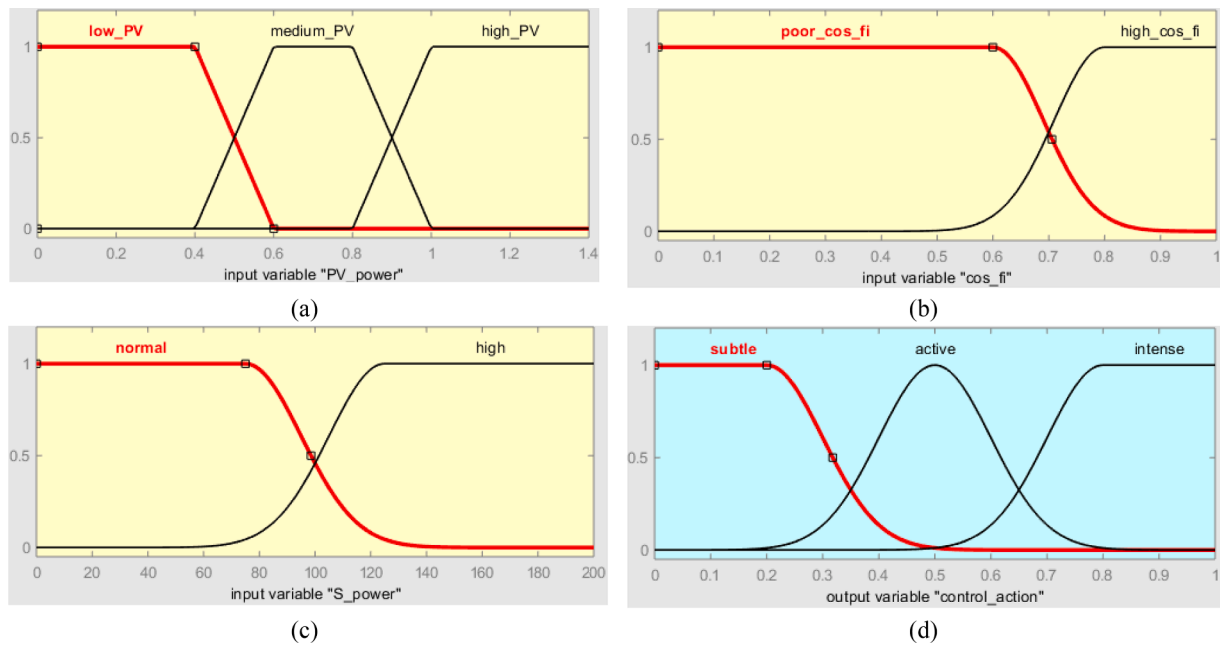


Fig. 7. Membership function plots: (a) PV generation; (b) power factor; (c) aggregated apparent power; (d) output of the tuning fuzzy logic controller.

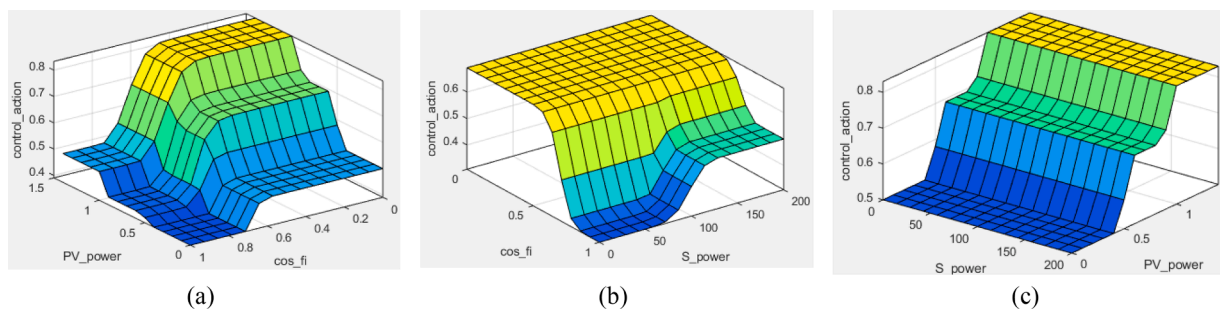


Fig. 8. Fuzzy control rule surfaces for the tuning system: (a) dependence of the output from the PV generation and the PF; (b) dependence of the output from the aggregated power and the PF; (c) dependence of the output from the PV generation and the aggregated power.

Table 3

Membership rules for the tuning part of the algorithm.

| IF the “PV power” is: | OR the “cosφ” is: | AND the “apparent power”: | THEN the Output is: |
|-----------------------|-------------------|---------------------------|---------------------|
| low                   | high              | –                         | subtle              |
| medium                | –                 | –                         | active              |
| high                  | poor              | –                         | intense             |
| low                   | –                 | high                      | intense             |
| medium                | –                 | high                      | intense             |
| –                     | high              | normal                    | subtle              |

higher harmonics is processed by the MATLAB S-function “s\_func\_calc\_thd,” which determines the voltage THD value. Information about the total transformer’s loading, THD, and ambient temperature is then sent to the fuzzy logic controller for diagnostics. Through the defuzzification process, according to the elaborated rules and MFs, crisp values for representing uncertain data are obtained. These values are translated to the scope “Status graph\_Function” and used to generate a warning message for a DSO. When the transformer is loaded more that 100% of its nameplate power, the load demand can be supported by the BESS (if activated).

The tuning part also has its fuzzy logic controller, which provides

input for three MATLAB functions responsible for tuning of the output of PV, SCB, and BESS. If the tuning part of the algorithm is activated, it determines the warning message for a DSO.

#### 4. Transformer’s aging model

The transformer’s aging is mainly related to the deterioration of winding’s insulation, which is a function of temperature, particularly winding hottest-spot temperature ( $\Theta_{HS}$ ) [36]:

$$\Theta_{HS,t} = \Theta_{A,t} + \Delta\theta_{O,t} + \Delta\theta_{HSO,t}, \tag{3}$$

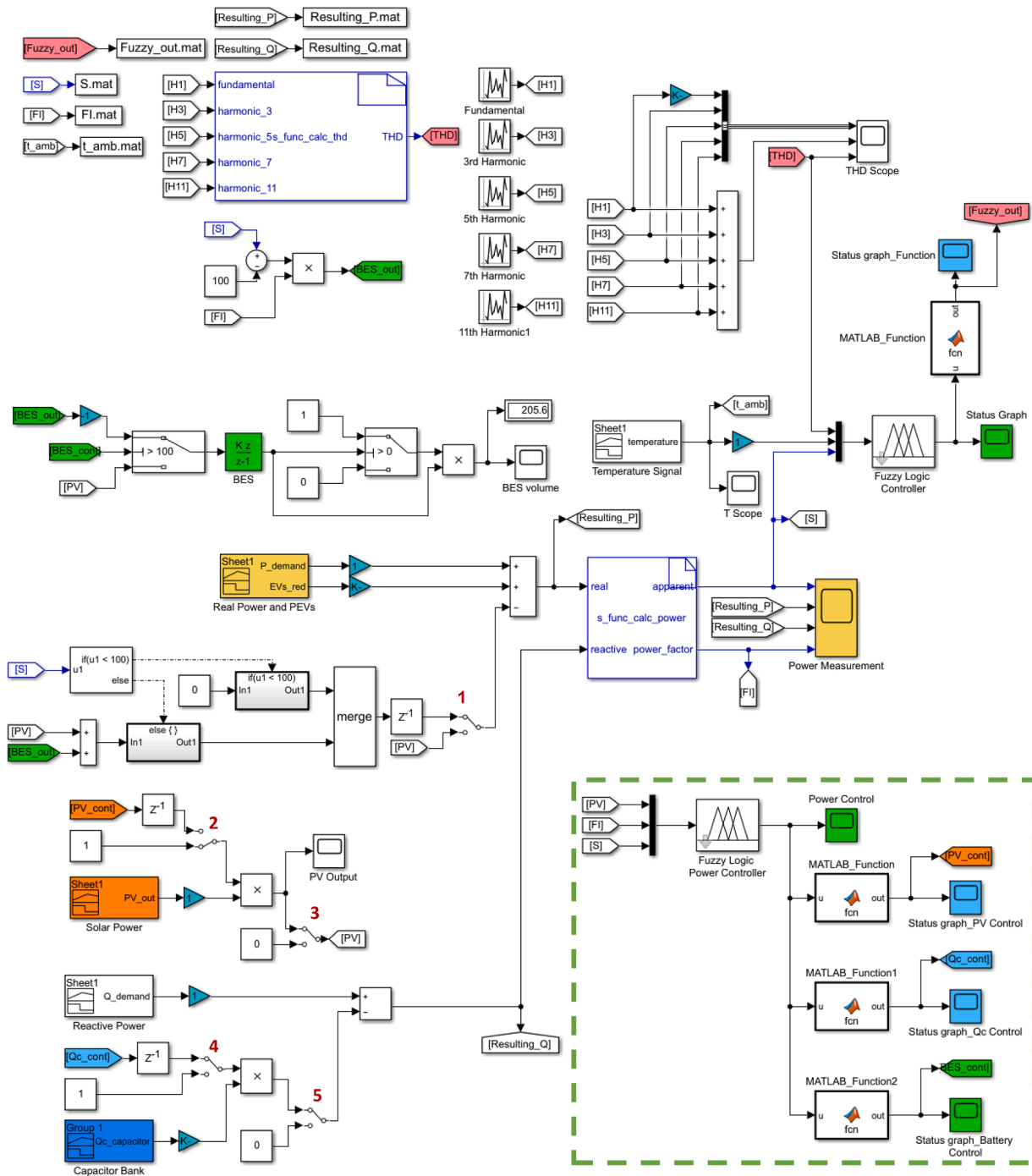


Fig. 9. The fuzzy-logic-based model in MATLAB-Simulink.

where  $\Theta_A$  is the temperature of the cooling medium (ambient temperature), °C;  $\Delta\theta_O$  is the transformer's top oil temperature (i.e. temperature in the upper layers) rise over the ambient temperature, °C;  $\Delta\theta_{HSO}$  is the transformer's hot-spot temperature rise over the top oil temperature, °C.

The coils' insulation degradation can be estimated with an index of degradation (such as LoL), which is used in the real transformer's thermal models [36–38].

It is assumed that the temperature rises  $\Delta\theta_{O,t}$  and  $\Delta\theta_{HSO,t}$  are independent of the temperature of the cooling medium in the range of its variation from +40 to –20 °C [38]. The dynamics of terms that characterize the temperature rise (i.e.,  $\Delta\theta_O$  and  $\Delta\theta_{HSO}$ ) depends on temperature changes in transient thermal processes and loading changes. In more detail the method of their calculation is presented in [29].

The transformer's relative wear is estimated using  $\Theta_{HS}$  by computing the aging acceleration factor [36]:

$$F_{AA} = e^{\left( \frac{15000}{\Theta_{HS}^{2.73}} - \frac{15000}{\Theta_{HS}^{ref\ 2.73}} \right)}, \quad (4)$$

where  $\Theta_{HS}^{ref}$  is the reference hottest-spot temperature, which is 110 °C for 65 °C average winding rise and 95 °C for 55 °C average winding rise transformers [36].

The aggregated relative wear for the given temperature cycle can be assessed with the equivalent aging factor, which is equal to the sum of the relative wear for all time intervals  $\Delta t_i$  ( $i = 1, 2 \dots M$ ) divided by the sum of time intervals:

$$F_{EqA} = \frac{\sum_{i=1}^M F_{AA,i} \cdot \Delta t_i}{\sum_{i=1}^M \Delta t_i}, \quad (5)$$

where  $F_{AA,i}$  is aging acceleration factor for the temperature that exists during  $\Delta t_i$ ;  $M$  is the total number of time intervals.

The yearly loss of life can be determined as follows:

$$LoL_y\% = \frac{F_{EqA} \cdot T}{L_N} \cdot 100, \quad (6)$$

where  $L_N$  is the insulation's normal life, which is equal to 180,000 h, according to [36],  $T$  is the period of time. For one year  $T = 8760$  h.

## 5. Simulation results and discussion

This section analyzes the simulation results for the electrical network, which operates under different EV penetration levels. The operating scenarios are as per Table 1. The transformers' aging is assessed and discussed.

The cumulative demand charts from residential and industrial consumers for different cases have been obtained during simulations. As an example, the cumulative charts aggregated at the 0.4 kV side for a winter weekday for the 100% EV penetration are shown in Fig. 10. The values in the ordinate axis were converted in p.u., using the transformer's rated power as the base, and are presented in percent. As it can be seen, the load profiles have a morning and an evening maximum. The curve 1 (in blue) is the aggregated demand at the secondary side of the transformer (base case), the curve 2 (in green) is the aggregated demand after the PV generation is deployed (case 1), the curve 3 (in gray) corresponds to the apparent power of the residential and the manufactural loads, and the dashed curve 4 (in brown) is the demand curve after the PV generation, the SCB, and the BESS have been added, which corresponds to the case 3 from Table 1.

Note that Fig. 10 only demonstrates the load profiles of a specific day for a reference purpose, and throughout the year these profiles are subjected to changes, according to the load demand and PV output data (see Section 2). Given that the household energy demand can be spatially and temporally variable, the EVs can have a greater or smaller relative effect on certain types of demand profiles. However, from the charts Fig. 10 it can be concluded that EV charging combined with

regular load demand is the most dangerous for the transformer at high EV penetration levels. Therefore, the transformer is the bottleneck of the considered distribution feeder; its capacity is likely to be exceeded at high EVs penetration, which will be further revealed in more detail.

Let us demonstrate the tuning effectiveness of the proposed method for the distribution transformer's aging mitigation on the example of the same working day under 100% EV penetration. As it had been stated earlier, the tuning process is successful if the duration of transformer's operation under more severe conditions is mitigated in favor to less severe conditions. The outputs of the fuzzy logic controllers for the base case and for the case 3, after tuning, are demonstrated in Fig. 11. As it can be seen, tuning allowed to reduce the duration of the most drastic operation mode (the integer 3 corresponds to the "Inevitable issue") in favor to the less adverse "Possible issue" mode (the crisp value 2).

Changes of the PF throughout the same winter day for different grid reinforcement scenarios, under 100% EV penetration, are demonstrated in Fig. 12. For the base case the average value of the PF is around 0.9. The corresponding curve is outlined with the blue crosses, and it is overlapped by other curves in many parts. As about the case 1, with addition of uncontrolled PV generation the PF drops down, with especially deep dip between 7:00 and 13:00. Activation of PV control for PF regulation can improve the PF, but in the time window between 7:00 and 13:00 it is still much lower than the desired value 0.92. Looking at the case 2, with addition of the non-regulated SCB the PF remains too low between 6:00 and 12:00, while during some time periods (e.g., from 15:00 till 2:00) it is close to unity. Activation of the tuning part of the model to control the SCB's reactive power output improves the PF only partially: it is still far from the desired value 0.92 during the large part of the day. The best values of the PF can be achieved with the case 3, when the electrical network is additionally reinforced with a controlled BESS.

Comprehensive results about the transformer's aging can be obtained from testing the algorithm on the yearly model for the considered demand profiles of the electrical network. The duration of the transformer's operation modes, according to the fuzzy logic output, the corresponding aggregated relative wear, and the LoL values for different EV penetration levels are summarized in Table 4. As it can be seen, there is a correlation between the duration of the most dangerous degrees of warning and the yearly LoL coefficients in percent. For 15%, 30%, and 50% EV penetration levels the charging loads have small impact on the transformer's deterioration, and the grid reinforcement strategies are not needed, since their effect is negligible. The combined influence of EVs charging and regular loads' demand (base case) is the most

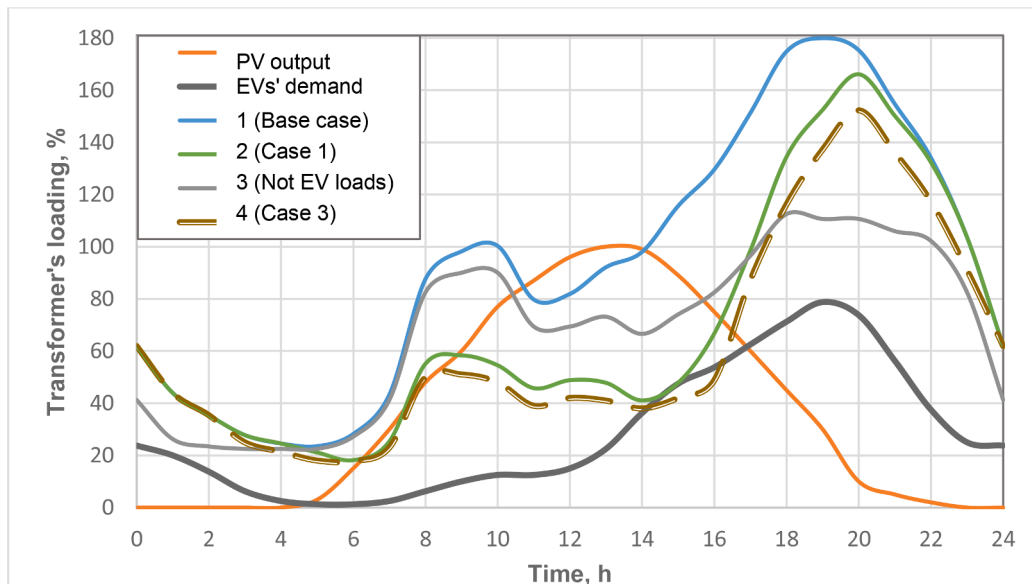


Fig. 10. Load demand profiles of the low-voltage distribution network under 100% EV penetration.

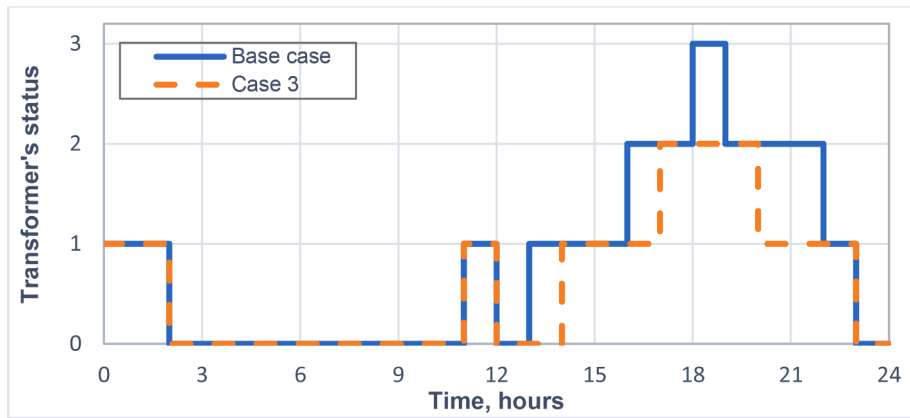


Fig. 11. Demonstration of transformer's operation tuning efficiency: base case vs. case 3 after diagnostics and tuning.

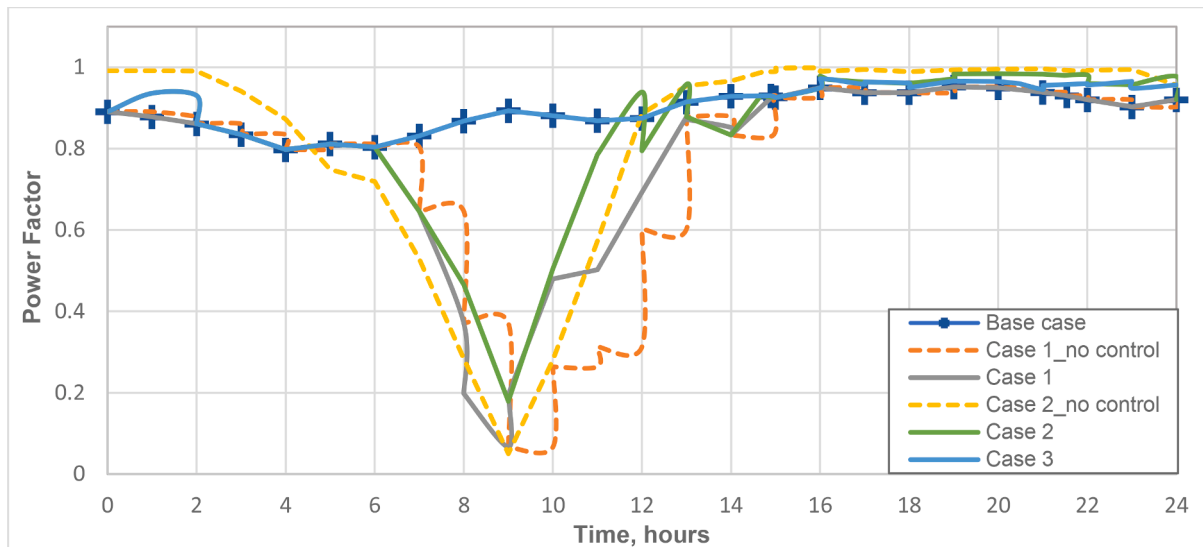


Fig. 12. Variations of the PF during a working day for different grid reinforcement cases, 100% EVs penetration.

devastating for the transformer: for the extreme 100% EV penetration the  $LoL_y$  reaches hazardous 31.43%, and for the 85% EV penetration the value of  $LoL_y$  is 8.13%. For the 67% EV penetration the loss of life is up to 1.67%, which is not very high for a mineral-oil-immersed transformer.

Injection of PV units (case 1) alleviates the aging just modestly: the PV generation has intermittent nature and usually makes its major contribution at noon, which coincides nor with the morning, nor with the evening demand peaks. Therefore, PV installations cannot be considered as a separate measure to mitigate the transformer's  $LoL$ , and their role is just supportive. A switched capacitor bank, which compensates the reactive power demand (case 2), allows to decrease the total apparent power, which results in notable lessening of the transformer's  $LoL_y$  by around 2 times for EV penetration levels 85% and above. Under lower EV penetrations the effect of the SCB is less notable.

A synergy of the controlled PV generation, SCB, and BESS (case 3) is the most resultive in terms of mitigation of the impact of EVs charging, ambient temperature, high power demand and harmonic distortions on the transformer's aging. The BESS would charge during the daytime from the PV generation, when there is no transformer's overloading. In the evenings, when most of the EVs are being recharged, community-level BESS and accumulation batteries of residential prosumers would send energy back to the houses or to the grid. In addition, the SCB installed on the transformer's secondary bus would compensate reactive power demand and help to maintain the PF at the desired level. This joint effect substantially reduces the transformer's loading and, as a

result, the  $LoL_y$  can be improved compared to the base case: 2.97 times for 67% EV penetration; 4.13 times for 85% EV penetration; 5.15 times for 100% EV penetration. As the result, the  $LoL_y$  for extreme EV penetration levels of 85% and 100% is mitigated to 1.97% and 6.1%, respectively. Although, the 6.1%  $LoL$  is a substantial value, the transformer's replacement can be delayed for a long time, if emergencies and long-duration overloading are avoided. Moreover, the case 3 demonstrates the most balanced composition of the degrees of warning. For instance, for 100% EV penetration the duration of the "Inevitable issue" status is only 87 h per year, while the mildest "No issue" status lasts for 2553 h, and the relatively harmless "Attention" status lasts for 3958 h. To compare, for the base case at 100% EV penetration the most dangerous status "Imminent problem" lasts for 295 h.

Summarizing, the case 3 is a preferable grid reinforcement strategy for development of electrical networks with high penetration of EVs and significant share of PV generation, which are similar to the network considered in this study. It allows to prolong the transformer's lifetime, while maintaining the PF near the desired value.

## 6. "Soft" strategies for improving the LOL of transformers

In the previous section several grid reinforcement technologies to mitigate the transformer's aging have been assessed. However, with proper management of EV charging, it is not only possible to avoid the negative consequences of additional load on the distribution network,

**Table 4**

The transformer's statuses and LoL for the whole year.

| Scenario  | EV penetration | Time duration of an output status, hours |           |                |                  | $F_{EqA}$ | $LoL_y\%$ |
|-----------|----------------|--|-----------|----------------|------------------|-----------|-----------|
|           |                | No issue                                 | Attention | Possible issue | Inevitable issue |           |           |
| Base case | 15%            | 3444.99                                  | 4582.98   | 732.03         | 0                | 0.0066    | 0.0319    |
| Case 1    |                | 3580.78                                  | 4586.82   | 592.40         | 0                | 0.0052    | 0.0252    |
| Case 2    |                | 3630.47                                  | 4572.29   | 557.24         | 0                | 0.0040    | 0.0195    |
| Case 3    |                | 3458.99                                  | 4599.65   | 701.37         | 0                | 0.0053    | 0.0259    |
| Base case | 33%            | 3097.51                                  | 4674.65   | 985.57         | 2.26             | 0.0223    | 0.1084    |
| Case 1    |                | 3275.67                                  | 4700.90   | 783.44         | 0                | 0.0195    | 0.0947    |
| Case 2    |                | 3342.99                                  | 4671.47   | 745.53         | 0                | 0.0124    | 0.0605    |
| Case 3    |                | 3140.13                                  | 4671.69   | 948.17         | 0.01             | 0.0141    | 0.0687    |
| Base case | 50%            | 2864.85                                  | 4546.33   | 1340.34        | 8.48             | 0.0764    | 0.3717    |
| Case 1    |                | 2893.19                                  | 4596.10   | 1262.24        | 8.47             | 0.0758    | 0.3687    |
| Case 2    |                | 3109.58                                  | 4568.14   | 1082.28        | 0                | 0.0477    | 0.2323    |
| Case 3    |                | 3161.57                                  | 4585.52   | 1012.91        | 0                | 0.0396    | 0.1928    |
| Base case | 67%            | 2698.18                                  | 4230.47   | 1810.95        | 20.41            | 0.3416    | 1.6625    |
| Case 1    |                | 2720.21                                  | 4375.49   | 1650.29        | 14               | 0.3278    | 1.5951    |
| Case 2    |                | 2972.03                                  | 4301.06   | 1481.1         | 5.8              | 0.2001    | 0.9736    |
| Case 3    |                | 3036.53                                  | 4339.98   | 1381.19        | 2.3              | 0.1155    | 0.5623    |
| Base case | 85%            | 2573.57                                  | 3907.22   | 2175.67        | 103.54           | 1.6711    | 8.1328    |
| Case 1    |                | 2885.94                                  | 3978.13   | 1821.57        | 74.36            | 1.6276    | 7.9210    |
| Case 2    |                | 2937.32                                  | 4052.25   | 1727.40        | 43.03            | 0.8582    | 4.1765    |
| Case 3    |                | 2595.29                                  | 4162.09   | 1965.37        | 37.25            | 0.4056    | 1.9738    |
| Base case | 100%           | 2543.82                                  | 3699.94   | 2221.05        | 295.19           | 6.4589    | 31.4335   |
| Case 1    |                | 2883.30                                  | 3797.65   | 1837.59        | 241.47           | 6.3371    | 30.8405   |
| Case 2    |                | 2915.68                                  | 3855.59   | 1833.58        | 155.15           | 3.2513    | 15.8232   |
| Case 3    |                | 2552.63                                  | 3957.64   | 2162.89        | 86.84            | 1.2537    | 6.1013    |

but even to increase the economic efficiency.

To shift the load associated with EV charging to off-peak times, several strategies are used [20,39]:

- Using of the vehicle-to-grid (V2G) technology.
- Introduction of time-of-use electricity rates for charging: EV owners who charge their vehicles during lower-demand times of day (usually overnight) are motivated by savings.
- Explaining tangible benefits of setting an automated off-peak charging schedule.
- Using of behavioral science techniques and personalization to educate customers on the impact of charging their EVs at different times of the day.

The essence of V2G technology is in the utilization of the batteries of parked EVs as energy storage units. In other words, EVs can take electricity from the grid during low demand periods, and then give it back to the grid at times of peak loads. Use of batteries of parked EVs as energy storage devices can help to reduce the required generation margin in the so-called hot standby, which in turn will reduce the need in expensive BESSs and contribute to a more economical operation of the electrical network. However, to implement the V2G, it is necessary to install charging stations supporting the reverse power flow.

As shown earlier, the probability of an unacceptable overload of a transformer is highly dependent on the EV penetration. In this regard, in

the networks with high EV penetration it is necessary to encourage users to recharge their vehicles during off-peak hours and participate in V2G. To do this, a flexible billing system can be used. To implement this, a tariff differentiated by zones of the day with a strong difference in price in each tariff zone can be established. Consumers respond to changes in the price of electricity by changing the demand. As the price rises, demand decreases, and vice versa, a decrease in price leads to an increase in demand. The level of consumer's response to a change in price is called the elasticity of demand [40]. The elasticity of demand is calculated with the following formula:

$$\varepsilon = \frac{\Delta W_{dem, \%}}{\Delta C, \%}, \quad (7)$$

where  $\Delta W_{dem, \%}$  is a change in electricity consumption associated with a change in its price;  $\Delta C, \%$  is the price change.

The report [40] shows that the average level of own-price elasticity of electricity demand in residential buildings in the United States is from  $-0.12$  in the short run to  $-0.29$  in the long run. Given that 80% of plug-in EVs recharging occurs at the residential homes [5], these values can be taken as a reference for the elasticity of the charging demand. Also, when modeling, the discreteness of the EVs charging load should be taken into account, that is, elasticity does not affect the load directly, but the number of users who want to charge their EVs at one time or another.

## 7. Conclusions

This study presents a fuzzy-logic-based framework to mitigate the aging of the transformer feeding a power distribution system with high penetration of plug-in EVs. Several negative factors affecting the transformers have been considered and incorporated in the model: ambient temperature, poor power quality, and overloads caused by excessive power demand from regular loads and EV charging. Effectiveness of following grid reinforcement methods to prevent unacceptable transformer's LoL has been evaluated: photovoltaic generation units, shunt capacitor banks, and battery energy storage systems, installed at the secondary voltage side.

The first part of the proposed algorithm makes diagnostics of the mineral-oil-immersed transformer's state and outputs a degree of warning (i.e., a message) for a distribution system operator. When the transformer's state corresponds to the "Inevitable issue", a distribution system operator should take actions to prevent a potential emergency. The second part (the tuning part) of the algorithm is aimed to avoid unacceptable overloading and maintain the power factor near the desired level. It can control the PV generation output, the shunt capacitor bank's output, and charging/discharging of the BESS. This part of the algorithm can be switched off by a user.

A clear dependence of the probability of unacceptable overload of the transformer and a decrease in its service life from the EV penetration level has been demonstrated. At 85% EV penetration, the charging loads combined with the regular load demand result in the transformer's loss of life of 8.13%, and at the ultimate 100% EV penetration the LoL reaches 31.43%, which will inevitably lead to a failure. Considering the grid reinforcement strategies, the best results can be observed when the electrical network is additionally equipped with controlled energy storage, PV installations and the shunt capacitor bank (i.e., case 3 of the study). For this case, at 100% EV penetration the transformer's LoL is reduced more than 5 times, compared to the base case. With this combined grid reinforcement strategy, it is possible to address the impact on the rising EV charging demand on the transformer's aging.

Despite the improvements in the LoL, the PF for the cases 1 and 2 remains unstable and often drops below the desired value. For the case 3 it is possible to maintain the PF closer to the desired value throughout the day.

The developed algorithm and the fuzzy-logic-based tool are universal and can be applied to any section of the electrical network if there is initial data on this section. In the future work the "soft" strategies for improving the LoL of transformers are to be considered, which include the scheduling of EV charging and the elasticity of demand.

### The evaluation of the authors' contribution

Illia Diahovchenko: creation of the research concept, developing of the mathematical model, research model development and simulation, analysis of the obtained results, manuscript preparation. Anastasiia Chuprun: research model development and simulation, manuscript preparation. Zsolt Čonka: reviewing.

### Declaration of Competing Interest

The authors declare that they have no known competing financial interests or personal relationships that could have appeared to influence the work reported in this paper.

### Data availability

Data will be made available on request.

## References

- [1] P. Ahmadi, Environmental impacts and behavioral drivers of deep decarbonization for transportation through electric vehicles, *J. Clean. Prod.* (2019).
- [2] R.K. Lattanzio and C.E. Clark, "Environmental effects of battery electric and internal combustion engine vehicles," Washington DC, United States, 2020.
- [3] "Global EV outlook 2022," 2022.
- [4] C.B. Jones, M. Lave, W. Vining, B.M. Garcia, Uncontrolled electric vehicle charging impacts on distribution electric power systems with primarily residential, commercial or industrial loads, *Energies* (2021).
- [5] G.P. Tal, D.P. Chakraborty, A.P. Jenn, J.H.P. Lee, D.P. Bunch, Factors affecting demand for plug-in charging infrastructure: an analysis of plug-in electric vehicle commuters, UC Off. Pres. ITS Rep. (2020).
- [6] P. Solberg, "Electric vehicles and charging stations in Europe," 2021.
- [7] V. Volokhin, I. Diahovchenko, V. Kurochkina, M. Kanálik, The influence of nonsinusoidal supply voltage on the amount of power consumption and electricity meter readings, *Energetika* 63 (1) (2017).
- [8] V.V. Volokhin, I.M. Diahovchenko, B.V. Derevyanko, Electric energy accounting and power quality in electric networks with photovoltaic power stations, in: Proceedings of the IEEE International Young Scientists Forum on Applied Physics and Engineering, YSF, 2017.
- [9] S. Seme, N. Lukač, B. Stumberger, M. Hadziselimović, Power quality experimental analysis of grid-connected photovoltaic systems in urban distribution networks, *Energy* (2017).
- [10] I. Diahovchenko, B. Dolník, M. Kanálik, J. Kurimský, Contemporary electric energy meters testing under simulated nonsinusoidal field conditions, *Electr. Eng.* 104 (2022) 1077–1092.
- [11] B.R. Klingenberg and P.F. Ribeiro, "Fuzzy logic application for time-varying harmonics," in *Time-Varying Waveform Distortions in Power Systems*, 2009.
- [12] V.V. Volokhin, I.M. Diahovchenko, B.V. Derevyanko, Prospects of nanomaterials use in current and voltage hall sensors to improve the measurements accuracy and reduce the external impacts, in: Proceedings of the IEEE 7th International Conference on Nanomaterials: Applications and Properties, NAP 2017-Janua, 2017.
- [13] S. Shevchenko, O. Dovgalyuk, D. Danylchenko, O. Rubanenko, S. Fedorchuk, A. Potryvai, Accounting for the effect of PV panel dustiness on system performance with correction for panel cleaning for matlab simulink, in: Proceedings of the IEEE 3rd Ukraine Conference on Electrical and Computer Engineering, UKRCON, 2021.
- [14] S. Fedorchuk, A. Ivakhnov, O. Bulhakov, D. Danylchenko, Optimization of storage systems according to the criterion of minimizing the cost of electricity for balancing renewable energy sources, in: Proceedings of the IEEE KhPI Week on Advanced Technology, KhPI Week Conference, 2020.
- [15] M. Müller, et al., Evaluation of grid-level adaptability for stationary battery energy storage system applications in Europe, *J. Energy Storage* (2017).
- [16] S. Argade, V. Aravinthan, W. Jewell, Probabilistic modeling of EV charging and its impact on distribution transformer loss of life, in: Proceedings of the IEEE International Electric Vehicle Conference, IEVC, 2012.
- [17] H.F.M. Mantilla, A. Pavaas, I.C. Durán, Aging of distribution transformers due to voltage harmonics, in: Proceedings of the 3rd IEEE Workshop on Power Electronics and Power Quality Applications, PEPQA, 2017.
- [18] T. Dao, B.T. Phung, Effects of voltage harmonic on losses and temperature rise in distribution transformers, *IET Gener. Transm. Distrib.* (2018).
- [19] P. Paevere, A. Higgins, Z. Ren, M. Horn, G. Grozev, C. McNamara, Spatio-temporal modelling of electric vehicle charging demand and impacts on peak household electrical load, *Sustain. Sci.* (2014).
- [20] A. VISAKH, M.P. SELVAN, Smart charging of electric vehicles to minimize the cost of charging and the rate of transformer aging in a residential distribution network, *Turk. J. Electr. Eng. Comput. Sci.* (2022).
- [21] N.B.G. Brinkel, W.L. Schram, T.A. AlSkaif, I. Lampropoulos, W.G.J.H.M. van Sark, Should we reinforce the grid? Cost and emission optimization of electric vehicle charging under different transformer limits, *Appl. Energy* (2020).
- [22] N. Shkitina, D. Akimov, Analysis of the influence of the stochastic load of electric vehicles on the distribution network, *Elektroener. Peredacha i Raspred.* 1 (20) (2021) 40–45.
- [23] H. Nafisi, Investigation on distribution transformer loss-of-life due to plug-in hybrid electric vehicles charging, *Int. J. Ambient Energy* (2021).
- [24] A. Palomino, M. Parvania, Data-driven risk analysis of joint electric vehicle and solar operation in distribution networks, *IEEE Open Access J. Power Energy* (2020).
- [25] C.M. Affonso, M. Kezunovic, Probabilistic assessment of electric vehicle charging demand impact on residential distribution transformer aging, in: Proceedings of the International Conference on Probabilistic Methods Applied to Power Systems, PMAPS, 2018.
- [26] A.A. Romero-Quete, E.E. Mombello, G. Rattá, Assessing the loss-of-insulation life of power transformers by estimating their historical loads and ambient temperature profiles using ANNs and Monte Carlo simulations, *Dyna* (2016) (Medellin).
- [27] L. He, L. Li, M. Li, Z. Li, X. Wang, A deep learning approach to the transformer life prediction considering diverse aging factors, *Front. Energy Res.* (2022).
- [28] S.A. El-Bataway, W.G. Morsi, Distribution transformer's loss of life considering residential prosumers owning solar shingles, high-power fast chargers and second-generation battery energy storage, *IEEE Trans. Ind. Inf.* (2019).
- [29] I. Diahovchenko, et al., Mitigation of transformers' loss of life in power distribution networks with high penetration of electric vehicles, *Results Eng.* 15 (2022), 100592. Sep.
- [30] Y.A. Schreider, G.J. Tee, A.G. Henney, The Monte Carlo method: the method of statistical trials, *Phys. Today* (1967).

- [31] J. Quirós-Tortós, L.(N) Ochoa, T. Butler, How electric vehicles and the grid work together, *IEEE Power Energy Mag.* (2018).
- [32] I. Diahovchenko, L. Petrichenko, I. Borzenkov, M. Kolcun, Application of photovoltaic panels in electric vehicles to enhance the range, *Heliyon* 8 (12) (2022) e12425.
- [33] Photovoltaic Geographical Information System (PVGIS), European Commission Joint Research Centre, 2022.
- [34] Foundations of Fuzzy Logic, MathWorks, Inc., 2022.
- [35] E.H. Mamdani, S. Assilian, An experiment in linguistic synthesis with a fuzzy logic controller, *Int. J. Man. Mach. Stud.* (1975).
- [36] IEEE Std. C57.91™-2011, IEEE guide for loading mineral- oil-immersed transformers and step-voltage regulators, in: *Proceedings of the IEEE Std C57.91™-2011(Revision C57.91-1995)*, 2011.
- [37] I.D. Voevodin, O.I. Sisunenکو, Timchenko, GOST 14209-85. General-Purpose Oil-Immersed Power transformers. Permissible loads, Standardinform, Moscow, 2009.
- [38] IEC, IEC 60076-7:2018. Power transformers - Part 7: loading guide for mineral-oil-immersed power transformers, 2nd ed. 2018.
- [39] J. Giampietro, Using Behavioral Techniques to Move Electric Vehicle Charging Off-Peak, Oracle Energy and Water Blog, 2022 [Online]. Available: <https://blogs.oracle.com/utilities/post/using-behavioral-techniques-to-move-electric-vehicle-charging-off-peak> [Accessed: 11-Mar-2023].
- [40] "Price elasticity for energy use in buildings in the United States," Washington, DC, 2021.